

Secondary Organic Aerosol Formation from Ambient Air at an Urban Site in Beijing: Effects of OH Exposure and Precursor Concentrations

Jun Liu,^{†,‡,Ⓞ} Biwu Chu,^{*,†,§,||} Tianzeng Chen,^{†,||} Changgeng Liu,^{†,#} Ling Wang,^{†,‡} Xiaolei Bao,^{†,⊥} and Hong He^{*,†,§,||}

[†]State Key Joint Laboratory of Environment Simulation and Pollution Control, Research Center for Eco-Environmental Sciences, Chinese Academy of Sciences, Beijing 100085, China

[‡]College of Environmental Science and Engineering, North China Electric Power University, Beijing 102206, China

[§]Center for Excellence in Regional Atmospheric Environment, Institute of Urban Environment, Chinese Academy of Sciences, Xiamen 361021, China

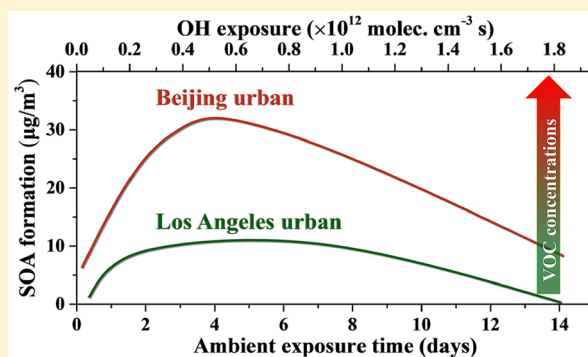
^{||}University of Chinese Academy of Sciences, Beijing 100049, China

[⊥]Hebei Provincial Academy of Environmental Sciences, Shijiazhuang 050051, China

[#]School of Resources and Environmental Engineering, Panzhihua University, Panzhihua 617000, China

Supporting Information

ABSTRACT: Secondary organic aerosol (SOA) is an important component of atmospheric fine particles (PM_{2.5}), while the key factors controlling SOA formation in ambient air remain poorly understood. In this work, the SOA formation in Beijing urban ambient air was investigated using an oxidation flow reactor (OFR) with high concentrations of OH radicals. The SOA formation potential increased significantly with the increase of ambient PM_{2.5} concentration during the observation. The optimum ambient exposure time, which is the aging time equivalent to atmospheric oxidation (with similar OH exposure) associated with the peak SOA formation, varied between 2 and 4 days in this study. The OA enhancement in this study was much higher than that of developed countries under different environmental conditions. The higher OA enhancement is probably due to the higher concentrations of volatile organic compounds (VOCs) in the urban air of Beijing. This might also have occurred because fragmentation did not dominate in the oxidation of OA, and did not result in negative OA enhancement on highly polluted days compared to relatively clean days with similar exposure time. These results suggested that under typical ambient conditions, high concentrations of VOC precursors might contribute to sustained organic aerosol growth and long duration haze events in Beijing.



INTRODUCTION

Organic aerosols (OA) account for a considerable proportion of ambient submicrometer aerosols in rural and urban areas, and have been the least-characterized species of aerosols owing to their diversity and complex atmospheric processes.¹ In order to comprehensively understand their impacts on human health, climate and visibility, it is essential to characterize their composition and source in detail.² However, knowledge about OA, including primary organic aerosols (POA) and secondary organic aerosols (SOA), is still limited.³ POA are mainly emitted into the atmosphere by anthropogenic sources, whereas SOA are primarily generated from the oxidation of volatile organic compounds (VOCs) by atmospheric oxidants and the further oxidation of POA.^{4–6} SOA have attracted increasing attention since they are an important component of fine particles (PM_{2.5}) in urban atmospheres. For instance, it was reported that OA account for 31–58% of the PM₁ mass concentration, of which 22–67% are SOA in urban Beijing.^{7–10}

In addition, the contribution of SOA to OA is greater during polluted days (63%) than clean days (35%) in Beijing.⁸ Thus, knowledge on SOA formation from urban air would shed light on further understanding its impacts on haze events.

Nowadays, studies on SOA formation are mainly performed by laboratory simulation,^{11,12} field observation,^{13,14} and model simulation.^{15,16} Although environmental chambers are widely used to investigate SOA formation, the significant wall losses of particles and semivolatile compounds in these chambers could affect the accuracy of the experimental results tremendously,^{17,18} especially over the long residence time (>1 day) typically required for studies in the chamber. In addition, SOA formation studies have mostly been performed under single

Received: November 7, 2017

Revised: May 14, 2018

Accepted: May 18, 2018

Published: May 18, 2018

VOC conditions.^{11,19} Therefore, the results obtained in the chamber would not accurately reflect the SOA formation at longer aging times in the atmosphere. In general, some models can be used to predict SOA concentrations based on the reported VOC oxidation mechanisms derived from laboratory studies. However, the present models cannot predict SOA formation accurately without adequate information on complex mixed VOC oxidation reaction systems.^{15,20}

To characterize SOA formation over a wide range of oxidant exposures, the potential aerosol mass (PAM) reactor was developed by Kang et al.^{21,22} The oxidation flow reactor (OFR) is a type of PAM, which introduces higher oxidant concentrations and OH exposure (up to 10^{12} molec. cm^{-3} s) than typical chambers, while having a short residence time (tens of seconds to a few minutes), and negligible wall losses. This allows the equivalent of longer ambient exposure times (hours to weeks) to be explored in both laboratory and field studies with the OFR. The SOA formation potential, defined as the maximum OA mass from the precursor gas oxidation process, has attracted increasing attention.^{13,21–23} Recent studies show that the SOA formation potential can be affected by oxidant concentration, presence of seed particles, type of VOC precursors, etc.^{12,22,24–27} However, most of these studies have focused on laboratory experiments, and more field experiments in complex environments (e.g., the urban atmosphere) are needed to gain further understanding of SOA formation. In a field study at a suburban site of Beijing, Chu et al.²⁸ found that local sources contributed more to SOA formation than air transported over long distances. Tkacik et al.²⁹ reported that mobile sources contribute about 2.9 ± 1.6 Tg SOA yr^{-1} in America, emphasizing the important contribution of SOA derived from vehicle exhaust to the particulate matter mass concentrations in urban areas, based on measurement of the SOA formation potential in a highway tunnel in Pittsburgh, PA. In the urban area of Los Angeles (LA), CA, field experimental results showed that the optimum ambient exposure time was 0.8–6 days and that the SOA formation potential was higher at night.¹³ These studies performed by OFR highlight the significance of the OFR in the study of SOA formation. However, few studies on the SOA formation potential of urban air have been reported, especially for polluted cities in developing countries.¹³ It is well-known that a large proportion of VOCs in urban environments are derived from anthropogenic emission sources, and would generate SOA with exposure to ambient air. Therefore, field experiments were carried out in this work to further understand the SOA formation of urban ambient air in Beijing. The SOA formation potential and related controlling factors of the urban air were investigated using an OFR.

■ EXPERIMENTAL SECTION

Sampling Setup in RCEES. The experiments were carried out during a 12-month period from August 2016 to August 2017 at a ground site located in the Research Center of Eco-Environmental Sciences (RCEES), CAS in Haidian district, Beijing, China. The station is 5 km northwest of the state-controlled air sampling site next to the National Olympic Sports Center, and could be considered as a typical urban environment. The OFR was mounted close to the wall on the second floor inside our laboratory, which is about 200 m away from Shuangqing Road, with no significant point source pollution nearby. The air sample injected into the OFR was transported from the roof inside a 25 mm diameter Teflon tube

(20 m in length) by a vacuum pump. Although only 6.8 L/min sample air was injected into the OFR, the flow rate of sample ambient air in the Teflon tube was about 200 L/min, so the residence time of air in the sample line was shortened to about 3 s to ensure minimal loss of the gas-phase pollutants. To some extent, the vapor losses of in-organic gases like SO_2 and NO_x in the sample tube can be considered negligible on the basis of comparison between our study and data from the field observation station in RCEES on the roof (see [Supporting Information \(SI\) Figure S1](#)). On the other hand, there might be significant inlet loss for low-volatility organic compounds (LVOCs). Unfortunately, we are not able to quantify this loss, which might cause an underestimation of the SOA formation potential in this study. Particle losses would be expected to occur in the nonconductive Teflon sample tube, but the effect of particle loss on the SOA formation potential was speculated to be slight and was not considered since this study focuses on the SOA formation potential derived from VOC oxidation. We admit the possibility of the loss of higher reactivity VOCs in our inlet system and in the mixing tube, even though we did our best to shorten the residence time of the air sample in the inlet. Particle loss should be irrefutably significant since a Teflon sampling tube was used. However, since we mainly focus on SOA formation from VOC oxidation, we think particle loss is a minor problem compared to gas pollutants with use of a bypass reactor as a reference. Although particle losses could take place in the sample tube, the SOA formation potential mainly derives from the oxidation of VOCs. Therefore, particle losses should have little effect on the SOA formation potential.

The OFR System. Following the design of the PAM reactor introduced by Kang et al.,^{21,22} two steel cylinder reactors constituting a twin-OFR were used to implement the experiment, as shown in [SI Figure S2](#). The volume of each cylinder reactor is about 15 L, with a length of 50 cm and diameter of 20 cm. Upstream of each reactor, a mixing tube with length of 30 cm and diameter of 6 cm is fixed to adequately mix inlet gases. The residence time of the air in the mixing tube is about 6 s, and the tube is made of stainless steel with FEP film coated on the inside surface. The inside walls of the reactors are coated with Teflon FEP film to reduce wall reactivity.²⁸ Four UV lamps (ZW20S26W, Beijing Lighting Research Institute, China) that mainly emit 254 nm light were installed in each reactor. During the experiments, the lamps of one reactor were turned on, and this reactor is referred to as the active reactor; while the lamps of the other reactor were turned off, and the reactor is referred to as the bypass reactor. In the field observation experiment, the air flow was switched between the two reactors every 30 min. Other than the lamps, the conditions of the two reactors remained consistent, including the temperature (T) and relative humidity (RH). Therefore, the wall losses were considered to be similar in the active reactor and bypass reactor, and did not have a significant effect on the calculation of SOA formation. The circulating cooling water (about 5 L/min) and zero air (about 2 L/min) constantly flowed in the interlayer around the reactors and UV lamps, respectively. The flow rates of the cooling water and zero air were controlled by mass flow controllers (MFC) to maintain the same temperature for the active and bypass reactors. T and RH were measured by temperature and humidity sensor probes, which were mounted near the outlet of the reactors. During the whole observation, T and RH were maintained in the specific ranges of 24–26 °C and 20–40%, respectively.

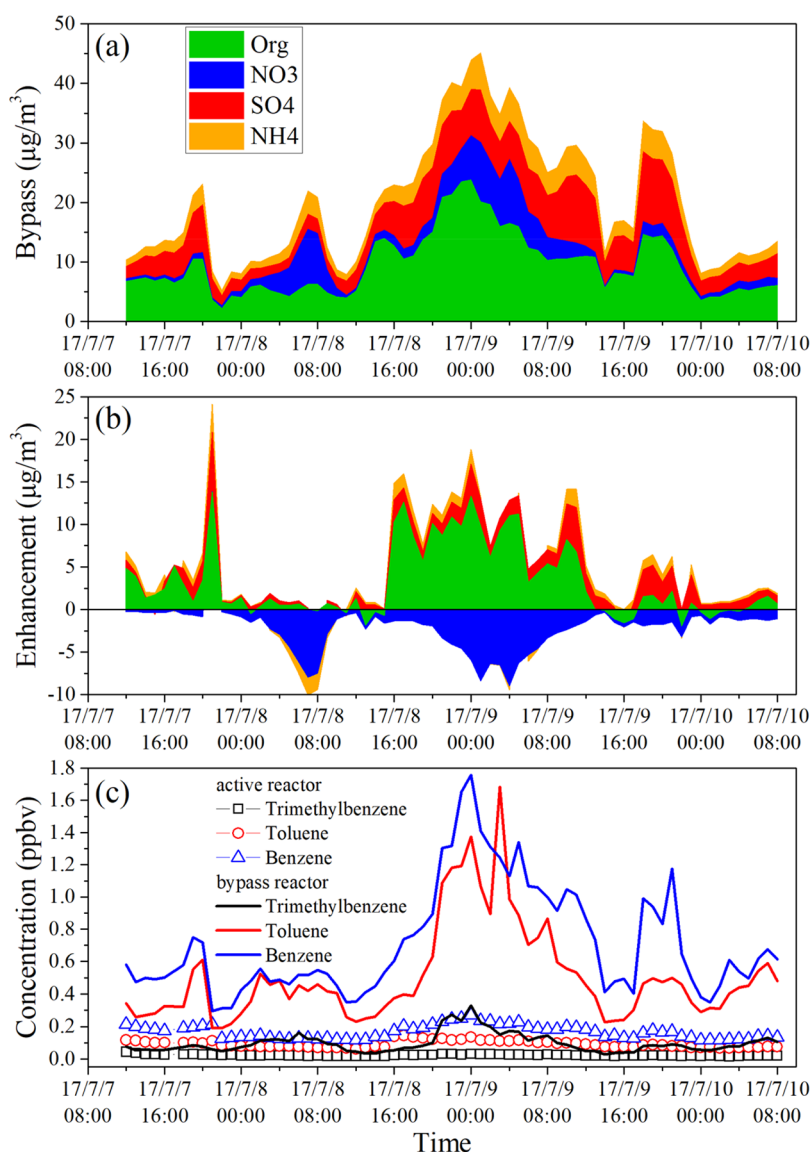


Figure 1. A typical time series of ambient aerosol (a), enhancement of OA (org), sulfate, nitrate and ammonium (b), three aromatic hydrocarbons in the bypass reactor and the active reactor (c) in the field observation experiment. Enhancement of OA is defined as the OA concentration in the active reactor minus that in the bypass reactor, $\text{OA}_{\text{active}} - \text{OA}_{\text{bypass}}$, i.e., SOA formation, and similar definitions are made for the enhancement of sulfate, nitrate, and ammonium.

Ambient air was mixed with humidified O₃ before entering the reactor. During field observation, the flow of O₃ was controlled at 1.2 L/min by a MFC, and was humidified by passing through an ultrapure water bubbler before entering the reactor. The inlet from OFR to AMS was dried by a diffusion drying tube. The internal OFR lights were kept constant and O₃ was generated by a homemade ozone generator in a specific concentration range by exposing the zero air to a 185 nm UV light (GPH 150T5L/4 and GPH 287T5L/4, UV-TEC Electronics Co., LTD, China). An exhaust pump and a MFC controlled the total flow rate at about 7.8 L/min (i.e., the flow rate of ambient air was about 6.6 L/min). The Reynolds number was calculated to be less than 100; even so, the residence time distribution of the oxidation flow reactor in this study, based on the design of the PAM reactor, is closer to Taylor dispersion flow rather than ideal laminar flow according to Lambe³⁰ and Huang.³¹ The direction of the total flow was controlled by an electromagnetic valve that determined which

reactor the fluid would pass through. OH radicals were generated by the photolysis of O₃ initiated by 254 nm UV light and subsequent reaction with H₂O. Each month, methanol or SO₂ was added into the reactor to characterize the OH exposure before the field observation experiments. In addition, the OH exposure was calibrated from the online decay of benzene and toluene monitored by a PTR-TOF-MS, following the method introduced by Ortega.³² The OH exposure estimated using benzene and toluene is shown in SI Figure S3. The final photochemical age used in this study was the average value of ages estimated from toluene and benzene.

The OH exposure is the integral of the OH radical concentration over the average residence time in the reactor, and the ambient exposure time represents the equivalent OH exposure time in the ambient atmosphere, assuming the 24 h average ambient OH radical concentration of 1.5×10^6 molecules cm^{-3} .³³ This value was used mainly due to

convenience of comparison with the literature. The OH concentration in Beijing might be higher than this value.

Instruments. The nonrefractory submicrometer aerosol at the reactor exit was quantitated by a high-resolution time-of-flight aerodyne aerosol mass spectrometer (HR-TOF-AMS). The concentrations of organic species, sulfate, nitrate, ammonium, and chloride, as well as the elemental composition of the organic aerosol, were measured every 3 min. Data were recorded as the 2 min average in “V mode” and 1 min average in “W mode”. Every month, the ionization efficiency was calibrated with 300 nm monodisperse, dried ammonium nitrate particles. A scanning mobility particle sizer (SMPS, TSI Inc., model 3082 with TSI 3776 CPC) was used to measure the PM₁ mass concentration with 5 min resolution. The gas-phase pollutants were measured by a set of gas monitors including a NO_x analyzer (42i, Thermo Fisher), SO₂ analyzer (43i, Thermo Fisher), CO analyzer (48i, Thermo Fisher) and O₃ analyzer (43i, Thermo Fisher). The PTR-TOF-MS was used to measure the concentration of VOCs with 5 min resolution. Calibrations for *m*-xylene, toluene and benzene were performed using standard gas before and after each experiment. The relative uncertainty for VOCs was estimated to be ±30%.

Comparison of the Results from Different Reactors. In order to verify the feasibility of using the OFR for this study, before the ambient observation experiment, SOA formation from *m*-xylene oxidation was compared with the previously reported results of another OFR. SI Figure S4 shows the results of SOA yield as a function of ambient exposure time in the two reactors. The experimental results reported by Lambe are very similar to the results of our reactors, both showing that the SOA yield first increased and then decreased as the ambient exposure time increased.³⁰ The maximum SOA yield of *m*-xylene oxidation in this OFR (0.10 ± 0.05) was close to the result of Lambe’s PAM (0.17 ± 0.08). The corresponding aging time equivalent to the atmospheric condition when SOA formation becomes maximized (hereafter referred to as the optimum ambient exposure time) in this study (about 2–4 days) was also close to that in Lambe’s experiment (about 2–3 days). Thus, it is feasible to compare the SOA formation and the subsequent aging process in our twin-OFR system to the previous studies.

RESULTS AND DISCUSSION

Time Variation of OA Enhancement and Correlation with Other Pollutants. SOA formation from ambient air at an urban site in Beijing was investigated in a 12-month period from August 2016 to August 2017. Figure 1 shows a typical variation trend of ambient aerosol, enhancement of OA and inorganic aerosols, and three aromatic hydrocarbons in the bypass reactor and the active reactor in 3 days of field experiments. OA enhancement (defined as the OA concentration difference between the active reactor and the bypass reactor, that is, $OA_{\text{active}} - OA_{\text{bypass}}$) showed a trend similar to bypass OA and bypass VOCs. The bypass species, including OA, nitrate, sulfate, ammonium, and three kinds of VOCs, showed the same trend, increasing or decreasing simultaneously. In Figure 1(b), the enhancement of OA and sulfate always remained positive, however, the nitrate was always negative, and ammonium varied with the relative concentrations of nitrate and sulfate. We attribute the nitrate decrease to the temperature gradient in the active reactor, in which high temperature near the lamps and low temperature near the wall (due to circulating cooling water) may cause more evaporation

and deposition on the wall. In order to identify the controlling factors for the SOA formation potential, the correlations between OA enhancement and some pollutants were further analyzed as shown in SI Figure S5. Figure S5 shows that OA enhancement and pollutants were positively correlated, with the best correlation for CO ($r^2 = 0.66$), suggesting that the increase of OA enhancement was closely related to the gradually elevated pollution level. The higher concentration of ambient VOCs in elevated pollution might result in the increase of OA enhancement. As shown in Figure 1, OA enhancement peaked at 16:00 on July 9, 2017. The VOC concentrations measured in the bypass reactor showed trends quite similar to OA enhancement, indicating the key role of VOC concentration in OA enhancement. The diurnal variations of OA enhancement and bypass benzene concentration are presented in Figure 2. Overall, higher OA enhancement at night and lower OA

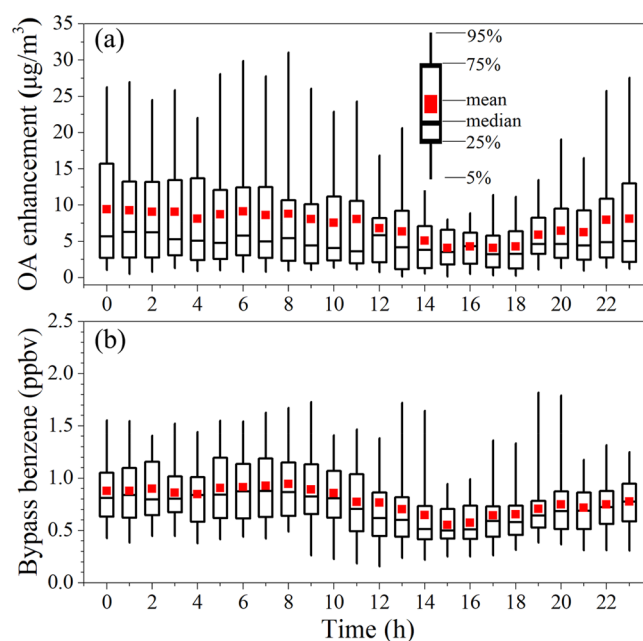


Figure 2. Diurnal variation of OA enhancement (a) and bypass benzene (b) in this study; red points: mean values of data groups; boxes show 25–75% data range, whiskers show 5–95% data range. Horizontal lines in boxes represent the median values of all data.

enhancement in daytime were observed, which is similar to the results of the field experiment in LA. The OA enhancement and bypass benzene seem to have the same diurnal variation. The lowest OA enhancement was observed at about 15:00, when the concentration of ozone reached its peak (SI Figure S6), which was also when the bypass benzene reached the lowest concentration. These results indicated the key role of ambient photochemical reactions in OA enhancement, which is consistent with a previous study showing higher OA enhancement at night rather than during the day.³³ The consumption of VOCs by ambient photooxidation cut down on the OA enhancement in the OFR significantly.

Effect of Ambient Exposure Time on OA Enhancement. The ambient exposure time has been considered to be a key factor in SOA formation in both laboratory and field studies.^{13,25} In order to study the effects of OH exposure on SOA formation, three controlled experiments on SOA formation at different pollution levels were carried out on March 18–21, 2017. The detailed experimental conditions and

Table 1. Experimental Conditions and Results of SOA Formation at Different Pollution Levels

exp. no.	date and time	prevailing wind direction	wind speed (m/s)	avg. bypass OA ($\mu\text{g}/\text{m}^3$)	avg. ambient $\text{PM}_{2.5}$ ($\mu\text{g}/\text{m}^3$)	avg. bypass benzene (ppbv)	peak of OA enhancement ($\mu\text{g}/\text{m}^3$)	optimum ambient exposure time (days)
1	2017.03.16/ 09:00–17:00	southwest	1–2	10.1 ± 2.0	134 ± 10	1.54 ± 0.24	30.2	4.2
2	2017.03.17/ 09:00–13:00	south	1–2	9.3 ± 1.6	120 ± 4	1.07 ± 0.21	20.8	4.0
3	2017.03.21/ 09:00–14:00	south	1–2	8.9 ± 1.1	99 ± 8	0.49 ± 0.09	7.1	2.5

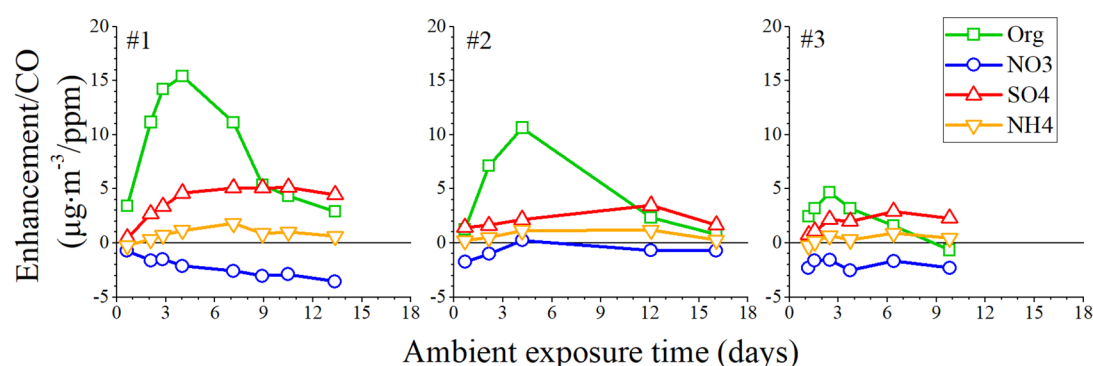


Figure 3. Normalized enhancement of OA, sulfate, nitrate, and ammonium as a function of the ambient exposure time with decreasing pollution levels in experiment nos. 1–3.

results are shown in Table 1. Although the air was quite polluted on all 3 days, there was a decreasing trend for the pollution level from experiment nos. 1–3. These three experiments were carried out when the meteorological conditions and pollution level were relatively stable, in order to maintain similar conditions during the experiment except for the stepwise increasing OH exposure. During these experiments, the ambient exposure time was changed by adjusting the concentration of O_3 in the OFR.

Figure 3 shows the variation of the enhancement of OA, sulfate, nitrate, and ammonium as a function of ambient exposure time. To reduce the effect of changing ambient conditions, the enhancement values were normalized with the observed CO concentrations. As the ambient exposure time increased, the OA enhancement first showed an increasing trend as the ambient exposure time increased to about 4 days (i.e., the optimum ambient exposure time), and then decreased as the ambient exposure time further increased. This change trend was the same as that found in previous studies.^{12,13,23,29}

Additional ambient exposure time decreased the SOA formation, probably due to fragmentation becoming more and more important relative to functionalization.^{27,29}

SOA formation increased as the bypass $\text{PM}_{2.5}$ concentration (or the pollution level, which was obtained from the state-controlled air observation site) increased (Figure 3). The higher concentrations of VOC precursors under higher pollution levels were oxidized and resulted in more SOA formation or more OA enhancement. In addition, SOA formation might become negative when the pollution level is not so severe, as seen for experiment no. 3 in Figure 3, but it stayed positive on more polluted days with similar or longer ambient exposure time. It can be inferred that VOC precursors can be oxidized to enter the regime where fragmentation dominates with long exposure time, which caused the ambient OA mass to decrease in the active reactor when lower VOC concentrations existed under less polluted conditions. During more polluted days, however, high concentrations of VOCs caused ambient OA to be harder to oxidize into the

fractionation-dominant regime, and the ambient OA did not show any negative enhancement even with long exposure time.

Table 2 shows the optimum ambient exposure time under different environmental conditions, including LA urban, pine

Table 2. Optimum Ambient Exposure Time and Maximum SOA Formation Reported in Previous Studies and the Experimental Results in This Study

object	ambient exposure time with the maximum SOA formation (days)	peak of OA enhancement ($\mu\text{g}/\text{m}^3$)
LA Urban air ¹³	0.8–6	~20
pine forest air ²³	0.4–1.5	~3
tunnel air ²⁹	2–3 ^a	~40
Beijing urban air (this study)	2–4	~30

^aOH exposure corrected by Ortega¹³ using the OH exposure estimation model of Peng.³⁴

forest and tunnel. The ambient exposure time with the maximum SOA formation and peak OA enhancement varied in different environmental conditions. The reason for this phenomenon might be that the properties and concentrations of VOC precursors in Beijing urban air are different from those under other environmental conditions. The concentrations of VOCs may play an important role in SOA formation.²² It turned out that the OA enhancement in Beijing was quite a bit larger than that in LA urban air and reached similar level of that in Tunnel air. As we mentioned earlier, the level of OA enhancement might still be underestimated due to the possible inlet loss of LVOCs in this study. The VOC concentrations from the tunnel experiment may be the highest, as inferred from the fact that it was performed during heavy traffic periods and in view of the poor ventilation in the tunnel. Higher OA enhancement was observed in the Beijing urban area than in LA; therefore, we suppose that the higher VOC concentrations in Beijing than LA would be the main reason. Although the detailed VOC concentrations in the Beijing urban area were not measured or available from the literature during the observation

period, higher VOC concentrations in Beijing than in LA could be speculated according to previous studies, which are listed in the SI (see Figure S7).^{35–38}

Besides their concentration, the reactivity of VOCs may also affect SOA formation. For example, MBO (2-methyl-3-buten-2-ol), methanol and monoterpenes were the most abundant VOCs in a pine forest.²³ The VOCs in the tunnel experiment were emitted by vehicles, with high concentrations of alkanes, alkenes and aromatic hydrocarbons.²⁹ These species also comprised the typical urban VOCs.^{7,39,40} Therefore, the OH reactivity of precursors should be considered to be an important factor that affects the optimum ambient exposure time under different environmental conditions. Monoterpenes and other biogenic VOCs, with C–C double bonds, have higher OH activity than alkanes. High concentrations of biogenic VOCs led to higher OH activity in pine forest air than in urban air and resulted in a lower optimum ambient exposure time. Similar optimum ambient exposure time was observed in Beijing as that in LA urban air and tunnel air, indicating a significant contribution of traffic emission to the VOCs in the Beijing urban area.

The Van Krevelen diagram of the entire observation period is shown in Figure 4. The ranges of the O/C and H/C ratios were

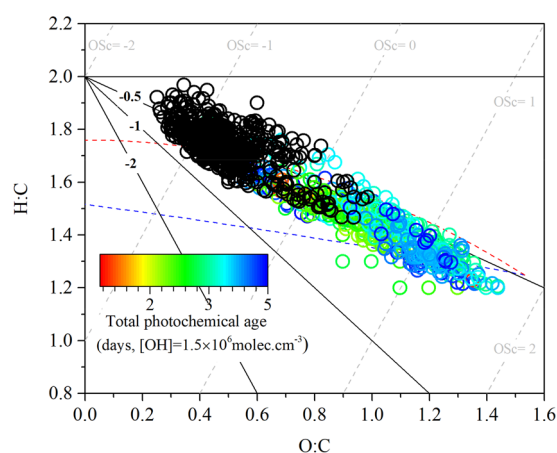


Figure 4. Van Krevelen diagram for bypass and active reactor measurements for entire sampling period. Black circles: data from bypass reactor, colored circles: active reactor.

0.3–1.4 and 1.2–2, respectively. The OSc and O/C ratios of organic aerosol in the active reactor increased with OH exposure time, while the H/C ratio decreased with OH exposure time. Similar change trends of these ratios in the bypass and active reactor implied that SOA produced in the active reactor had similar compositions to those of SOA in the ambient atmosphere. In addition, SI Figure S8 shows the results of O/C ratio, H/C ratio and OSc as a function of photochemical age. Their change trends are consistent with the results of the observation in the LA area.¹³ The maximum OSc in this study is smaller than that in the LA area, which could have resulted from the relatively shorter photochemical age and also the higher concentrations of OA and VOCs of this study. The H/C ratio of ambient aerosol was close to 2, corresponding to alkenes or cycloalkanes, and this might be ascribed to fresh POA emission.⁴¹

Atmospheric Implications. This study investigated the SOA formation of Beijing urban ambient air using an OFR. Considering the complicated chemical compositions and

characteristics of VOCs in urban environmental air, the OFR could be employed as a useful tool to characterize VOC pollution, since SOA formation increased with increasing VOC concentrations. In the Beijing urban environment, the OA enhancement is relatively higher than similar urban environments in developed countries. It was assumed that this difference resulted from the higher concentrations of VOCs in Beijing urban air than in other areas. Compared to relatively less-polluted days, the ambient OA is relatively hard to oxidize into the regime where fragmentation dominates, and rarely resulted in a mass decrease with similar exposure time under the severe pollution conditions in Beijing. These results suggested that under polluted ambient conditions, high concentrations of VOC precursors might contribute to sustained organic aerosol (OA) growth and the long duration haze events in Beijing.

■ ASSOCIATED CONTENT

📄 Supporting Information

The Supporting Information is available free of charge on the ACS Publications website at DOI: 10.1021/acs.est.7b05701.

Additional details on the schematic and feasibility analysis of the OFR in field experiment, correlations analysis between OA enhancement and other pollutants, estimation method of photochemical age, elemental composition of organic aerosol and comparison of VOC compositions (PDF)

■ AUTHOR INFORMATION

Corresponding Authors

*(C.B.W.) Phone: (+86)-010-62849337; e-mail: bwchu@rcees.ac.cn.

*(H.H.) Phone: (+86)-010-62849123; e-mail: honghe@rcees.ac.cn.

ORCID

Jun Liu: 0000-0002-3065-799X

Notes

The authors declare no competing financial interest.

■ ACKNOWLEDGMENTS

This work was financially supported by the National Key R&D Program of China (2016YFC0202700), the Youth Innovation Promotion Association, CAS (2018060), and the Strategic Priority Research Program of the Chinese Academy of Sciences (XDB05010300).

■ REFERENCES

- (1) Jimenez, J. L.; Canagaratna, M. R.; Donahue, N. M.; Prevot, A. S. H.; Zhang, Q.; Kroll, J. H.; DeCarlo, P. F.; Allan, J. D.; Coe, H.; Ng, N. L.; Aiken, A. C.; Docherty, K. S.; Ulbrich, I. M.; Grieshop, A. P.; Robinson, A. L.; Duplissy, J.; Smith, J. D.; Wilson, K. R.; Lanz, V. A.; Hueglin, C.; Sun, Y. L.; Tian, J.; Laaksonen, A.; Raatikainen, T.; Rautiainen, J.; Vaattovaara, P.; Ehn, M.; Kulmala, M.; Tomlinson, J. M.; Collins, D. R.; Cubison, M. J.; Dunlea, E. J.; Huffman, J. A.; Onasch, T. B.; Alfarra, M. R.; Williams, P. I.; Bower, K.; Kondo, Y.; Schneider, J.; Drewnick, F.; Borrmann, S.; Weimer, S.; Demerjian, K.; Salcedo, D.; Cottrell, L.; Griffin, R.; Takami, A.; Miyoshi, T.; Hatakeyama, S.; Shimojo, A.; Sun, J. Y.; Zhang, Y. M.; Dzepina, K.; Kimmel, J. R.; Sueper, D.; Jayne, J. T.; Herndon, S. C.; Trimborn, A. M.; Williams, L. R.; Wood, E. C.; Middlebrook, A. M.; Kolb, C. E.; Baltensperger, U.; Worsnop, D. R. Evolution of organic aerosols in the atmosphere. *Science* **2009**, 326 (5959), 1525–1529.

- (2) Kanakidou, M.; Seinfeld, J. H.; Pandis, S. N.; Barnes, I.; Dentener, F. J.; Facchini, M. C.; Van Dingenen, R.; Ervens, B.; Nenes, A.; Nielsen, C. J.; Swietlicki, E.; Putaud, J. P.; Balkanski, Y.; Fuzzi, S.; Horth, J.; Moortgat, G. K.; Winterhalter, R.; Myhre, C. E. L.; Tsigaridis, K.; Vignati, E.; Stephanou, E. G.; Wilson, J. Organic aerosol and global climate modelling: a review. *Atmos. Chem. Phys.* **2005**, *5*, 1053–1123.
- (3) Kroll, J. H.; Seinfeld, J. H. Chemistry of secondary organic aerosol: Formation and evolution of low-volatility organics in the atmosphere. *Atmos. Environ.* **2008**, *42* (16), 3593–3624.
- (4) Pankow, J. F. An absorption-model of gas-particle partitioning of organic-compounds in the atmosphere. *Atmos. Environ.* **1994**, *28* (2), 185–188.
- (5) Donahue, N. M.; Robinson, A. L.; Stanier, C. O.; Pandis, S. N. Coupled partitioning, dilution, and chemical aging of semivolatile organics. *Environ. Sci. Technol.* **2006**, *40* (8), 2635–2643.
- (6) Ervens, B.; Turpin, B. J.; Weber, R. J. Secondary organic aerosol formation in cloud droplets and aqueous particles (aqSOA): a review of laboratory, field and model studies. *Atmos. Chem. Phys.* **2011**, *11* (21), 11069–11102.
- (7) Sun, J.; Wu, F. K.; Hu, B.; Tang, G. Q.; Zhang, J. K.; Wang, Y. S. VOC characteristics, emissions and contributions to SOA formation during hazy episodes. *Atmos. Environ.* **2016**, *141*, 560–570.
- (8) Zhang, J. K.; Sun, Y.; Liu, Z. R.; Ji, D. S.; Hu, B.; Liu, Q.; Wang, Y. S. Characterization of submicron aerosols during a month of serious pollution in Beijing, 2013. *Atmos. Chem. Phys.* **2014**, *14* (6), 2887–2903.
- (9) Sun, Y. L.; Jiang, Q.; Wang, Z. F.; Fu, P. Q.; Li, J.; Yang, T.; Yin, Y. Investigation of the sources and evolution processes of severe haze pollution in Beijing in January 2013. *J. Geophys. Res.-Atmos.* **2014**, *119* (7), 4380–4398.
- (10) Sun, Y. L.; Wang, Z. F.; Dong, H. B.; Yang, T.; Li, J.; Pan, X. L.; Chen, P.; Jayne, J. T. Characterization of summer organic and inorganic aerosols in Beijing, China with an Aerosol Chemical Speciation Monitor. *Atmos. Environ.* **2012**, *51*, 250–259.
- (11) Zhao, R.; Aljawhary, D.; Lee, A. K. Y.; Abbatt, J. P. D. Rapid aqueous-phase photooxidation of dimers in the alpha-pinene secondary organic aerosol. *Environ. Sci. Technol. Lett.* **2017**, *4* (6), 205–210.
- (12) Lambe, A. T.; Onasch, T. B.; Croasdale, D. R.; Wright, J. P.; Martin, A. T.; Franklin, J. P.; Massoli, P.; Kroll, J. H.; Canagaratna, M. R.; Brune, W. H.; Worsnop, D. R.; Davidovits, P. Transitions from functionalization to fragmentation reactions of laboratory secondary organic aerosol (SOA) generated from the OH oxidation of alkane precursors. *Environ. Sci. Technol.* **2012**, *46* (10), 5430–5437.
- (13) Ortega, A. M.; Hayes, P. L.; Peng, Z.; Palm, B. B.; Hu, W. W.; Day, D. A.; Li, R.; Cubison, M. J.; Brune, W. H.; Graus, M.; Warneke, C.; Gilman, J. B.; Kuster, W. C.; de Gouw, J.; Gutierrez-Montes, C.; Jimenez, J. L. Real-time measurements of secondary organic aerosol formation and aging from ambient air in an oxidation flow reactor in the Los Angeles area. *Atmos. Chem. Phys.* **2016**, *16* (11), 7411–7433.
- (14) Xu, W.; Han, T.; Du, W.; Wang, Q.; Chen, C.; Zhao, J.; Zhang, Y.; Li, J.; Fu, P.; Wang, Z.; Worsnop, D. R.; Sun, Y. Effects of aqueous-phase and photochemical processing on secondary organic aerosol formation and evolution in Beijing, China. *Environ. Sci. Technol.* **2017**, *51* (2), 762–770.
- (15) Hu, J. L.; Wang, P.; Ying, Q.; Zhang, H. L.; Chen, J. J.; Ge, X. L.; Li, X. H.; Jiang, J. K.; Wang, S. X.; Zhang, J.; Zhao, Y.; Zhang, Y. Y. Modeling biogenic and anthropogenic secondary organic aerosol in China. *Atmos. Chem. Phys.* **2017**, *17* (1), 77–92.
- (16) Hayes, P. L.; Carlton, A. G.; Baker, K. R.; Ahmadov, R.; Washenfelder, R. A.; Alvarez, S.; Rappengluck, B.; Gilman, J. B.; Kuster, W. C.; de Gouw, J. A.; Zotter, P.; Prevot, A. S. H.; Szidat, S.; Kleindienst, T. E.; Offenberg, J. H.; Ma, P. K.; Jimenez, J. L. Modeling the formation and aging of secondary organic aerosols in Los Angeles during CalNex 2010. *Atmos. Chem. Phys.* **2015**, *15* (10), 5773–5801.
- (17) Zhang, X.; Cappa, C. D.; Jathar, S. H.; McVay, R. C.; Ensberg, J. J.; Kleeman, M. J.; Seinfeld, J. H. Influence of vapor wall loss in laboratory chambers on yields of secondary organic aerosol. *Proc. Natl. Acad. Sci. U. S. A.* **2014**, *111* (16), 5802–5807.
- (18) Krechmer, J. E.; Coggon, M. M.; Massoli, P.; Nguyen, T. B.; Crounse, J. D.; Hu, W.; Day, D. A.; Tyndall, G. S.; Henze, D. K.; Rivera-Rios, J. C.; Nowak, J. B.; Kimmel, J. R.; Mauldin, R. L., 3rd; Stark, H.; Jayne, J. T.; Sipila, M.; Junninen, H.; Clair, J. M.; Zhang, X.; Feiner, P. A.; Zhang, L.; Miller, D. O.; Brune, W. H.; Keutsch, F. N.; Wennberg, P. O.; Seinfeld, J. H.; Worsnop, D. R.; Jimenez, J. L.; Canagaratna, M. R. Formation of low volatility organic compounds and secondary organic aerosol from isoprene hydroxyhydroperoxide low-NO oxidation. *Environ. Sci. Technol.* **2015**, *49* (17), 10330–10339.
- (19) Tuet, W. Y.; Chen, Y. L.; Xu, L.; Fok, S.; Gao, D.; Weber, R. J.; Ng, N. L. Chemical oxidative potential of secondary organic aerosol (SOA) generated from the photooxidation of biogenic and anthropogenic volatile organic compounds. *Atmos. Chem. Phys.* **2017**, *17* (2), 839–853.
- (20) Li, J. L.; Zhang, M. G.; Wu, F. K.; Sun, Y. L.; Tang, G. G. Assessment of the impacts of aromatic VOC emissions and yields of SOA on SOA concentrations with the air quality model RAMS-CMAQ. *Atmos. Environ.* **2017**, *158*, 105–115.
- (21) Kang, E.; Root, M. J.; Toohey, D. W.; Brune, W. H. Introducing the concept of Potential Aerosol Mass (PAM). *Atmos. Chem. Phys.* **2007**, *7* (22), 5727–5744.
- (22) Kang, E.; Toohey, D. W.; Brune, W. H. Dependence of SOA oxidation on organic aerosol mass concentration and OH exposure: experimental PAM chamber studies. *Atmos. Chem. Phys.* **2011**, *11* (4), 1837–1852.
- (23) Palm, B. B.; Campuzano-Jost, P.; Ortega, A. M.; Day, D. A.; Kaser, L.; Jud, W.; Karl, T.; Hansel, A.; Hunter, J. F.; Cross, E. S.; Kroll, J. H.; Peng, Z.; Brune, W. H.; Jimenez, J. L. In situ secondary organic aerosol formation from ambient pine forest air using an oxidation flow reactor. *Atmos. Chem. Phys.* **2016**, *16* (5), 2943–2970.
- (24) Li, R.; Palm, B. B.; Borbon, A.; Graus, M.; Warneke, C.; Ortega, A. M.; Day, D. A.; Brune, W. H.; Jimenez, J. L.; de Gouw, J. A. Laboratory studies on secondary organic aerosol formation from crude oil vapors. *Environ. Sci. Technol.* **2013**, *47* (21), 12566–12574.
- (25) Lambe, A. T.; Chhabra, P. S.; Onasch, T. B.; Brune, W. H.; Hunter, J. F.; Kroll, J. H.; Cummings, M. J.; Brogan, J. F.; Parmar, Y.; Worsnop, D. R.; Kolb, C. E.; Davidovits, P. Effect of oxidant concentration, exposure time, and seed particles on secondary organic aerosol chemical composition and yield. *Atmos. Chem. Phys.* **2015**, *15* (6), 3063–3075.
- (26) Li, R.; Palm, B. B.; Ortega, A. M.; Hlywiak, J.; Hu, W.; Peng, Z.; Day, D. A.; Knote, C.; Brune, W. H.; de Gouw, J. A.; Jimenez, J. L. Modeling the radical chemistry in an oxidation flow reactor: radical formation and recycling, sensitivities, and the OH exposure estimation equation. *J. Phys. Chem. A* **2015**, *119* (19), 4418–4432.
- (27) Hall, W. A. T.; Pennington, M. R.; Johnston, M. V. Molecular transformations accompanying the aging of laboratory secondary organic aerosol. *Environ. Sci. Technol.* **2013**, *47* (5), 2230–2237.
- (28) Chu, B.; Liu, Y.; Ma, Q.; Ma, J.; He, H.; Wang, G.; Cheng, S.; Wang, X. Distinct potential aerosol masses under different scenarios of transport at a suburban site of Beijing. *J. Environ. Sci. (Beijing, China)* **2016**, *39*, 52–61.
- (29) Tkacik, D. S.; Lambe, A. T.; Jathar, S.; Li, X.; Presto, A. A.; Zhao, Y.; Blake, D.; Meinardi, S.; Jayne, J. T.; Croteau, P. L.; Robinson, A. L. Secondary organic aerosol formation from in-use motor vehicle emissions using a potential aerosol mass reactor. *Environ. Sci. Technol.* **2014**, *48* (19), 11235–11242.
- (30) Lambe, A. T.; Ahern, A. T.; Williams, L. R.; Slowik, J. G.; Wong, J. P. S.; Abbatt, J. P. D.; Brune, W. H.; Ng, N. L.; Wright, J. P.; Croasdale, D. R.; Worsnop, D. R.; Davidovits, P.; Onasch, T. B. Characterization of aerosol photooxidation flow reactors: heterogeneous oxidation, secondary organic aerosol formation and cloud condensation nuclei activity measurements. *Atmos. Meas. Tech.* **2011**, *4* (3), 445–461.
- (31) Huang, Y. L.; Coggon, M. M.; Zhao, R.; Lignell, H.; Bauer, M. U.; Flagan, R. C.; Seinfeld, J. H. The Caltech Photooxidation Flow

Tube reactor: design, fluid dynamics and characterization. *Atmos. Meas. Tech.* **2017**, *10* (3), 839–867.

(32) Ortega, A. M.; Day, D. A.; Cubison, M. J.; Brune, W. H.; Bon, D.; de Gouw, J. A.; Jimenez, J. L. Secondary organic aerosol formation and primary organic aerosol oxidation from biomass-burning smoke in a flow reactor during FLAME-3. *Atmos. Chem. Phys.* **2013**, *13* (22), 11551–11571.

(33) Mao, J.; Ren, X.; Brune, W. H.; Olson, J. R.; Crawford, J. H.; Fried, A.; Huey, L. G.; Cohen, R. C.; Heikes, B.; Singh, H. B.; Blake, D. R.; Sachse, G. W.; Diskin, G. S.; Hall, S. R.; Shetter, R. E. Airborne measurement of OH reactivity during INTEX-B. *Atmos. Chem. Phys.* **2009**, *9* (1), 163–173.

(34) Peng, Z.; Day, D. A.; Stark, H.; Li, R.; Lee-Taylor, J.; Palm, B. B.; Brune, W. H.; Jimenez, J. L. HOx radical chemistry in oxidation flow reactors with low-pressure mercury lamps systematically examined by modeling. *Atmos. Meas. Tech.* **2015**, *8* (11), 4863–4890.

(35) Baker, A. K.; Beyersdorf, A. J.; Doezema, L. A.; Katzenstein, A.; Meinardi, S.; Simpson, I. J.; Blake, D. R.; Rowland, F. S. Measurements of nonmethane hydrocarbons in 28 United States cities. *Atmos. Environ.* **2008**, *42* (1), 170–182.

(36) Duan, J. C.; Tan, J. H.; Yang, L.; Wu, S.; Hao, J. M. Concentration, sources and ozone formation potential of volatile organic compounds (VOCs) during ozone episode in Beijing. *Atmos. Res.* **2008**, *88* (1), 25–35.

(37) Li, J.; Wu, R.; Li, Y.; Hao, Y.; Xie, S.; Zeng, L. Effects of rigorous emission controls on reducing ambient volatile organic compounds in Beijing, China. *Sci. Total Environ.* **2016**, *557–558*, 531–541.

(38) Pang, Y. B.; Fuentes, M.; Rieger, P. Trends in selected ambient volatile organic compound (VOC) concentrations and a comparison to mobile source emission trends in California's south coast air basin. *Atmos. Environ.* **2015**, *122*, 686–695.

(39) Borbon, A.; Gilman, J. B.; Kuster, W. C.; Grand, N.; Chevaillier, S.; Colomb, A.; Dolgorouky, C.; Gros, V.; Lopez, M.; Sarda-Esteve, R.; Holloway, J.; Stutz, J.; Petetin, H.; McKeen, S.; Beekmann, M.; Warneke, C.; Parrish, D. D.; de Gouw, J. A. Emission ratios of anthropogenic volatile organic compounds in northern mid-latitude megacities: Observations versus emission inventories in Los Angeles and Paris. *J. Geophys. Res.-Atmos.* **2013**, *118* (4), 2041–2057.

(40) Li, L. Y.; Xie, S. D.; Zeng, L. M.; Wu, R. R.; Li, J. Characteristics of volatile organic compounds and their role in ground-level ozone formation in the Beijing-Tianjin-Hebei region, China. *Atmos. Environ.* **2015**, *113*, 247–254.

(41) Heald, C. L.; Kroll, J. H.; Jimenez, J. L.; Docherty, K. S.; DeCarlo, P. F.; Aiken, A. C.; Chen, Q.; Martin, S. T.; Farmer, D. K.; Artaxo, P. A simplified description of the evolution of organic aerosol composition in the atmosphere. *Geophys. Res. Lett.* **2010**, *37*, 5.